PROC 6TH EUROPEAN TURBOMACHINERY CONF.
LILLE, FRANCE, 2005
VOL 2, pp 1085-1095
EDS. G. BOIS, C. SIEVERDING, M. MANNA, T. ARTS

103_04/186

LINER OPTIMIZATION USING A HYBRID FINITE ELEMENT METHOD

L. Lafronza, W. Song, A. McAlpine, R.J. Astley and A.J. Keane

Computational Engineering Design Group and
Institute of Sound and Vibration Research,
University of Southampton, Southampton SO17 1BJ, UK.
lorenzo@soton.ac.uk

ABSTRACT

This paper makes use of a novel finite element method for aeroacoustics analysis to examine and optimise the design of liners for aeroengine inlets. The finite element approximation used is very efficient since it allows the treatment of non-axisymmetric nacelles by combining a standard bi-quadratic approximation in the axial and radial directions, with a spectral representation in the circumferential direction. Results from the code are used in a multi-fidelity optimization approach which is based on response surface and formal design of experiment methods. The design optimization also makes use of Grid computing technology to allow efficient use of computational resources and effective management of the analysis results. The use of these various techniques in combination allows for significant improvements to liner designs with realistic geometries at modest computational cost.

NOMENCLATURE

ρ	base flow density, kg/m^3
c	speed of sound, m/s
ϕ	steady velocity potential
$\widehat{\phi}$	linear potential fluctuation << $\|\phi\|$
m	azimuthal mode number
B	number of fan blades
b	duct radius, m
L	total axial liner length, m
M_x	Mach number
f	excitation frequency, Hz
ω	angular frequency $\omega = 2\pi f$, rad/s
EO	engine order
BPF	blade passing frequency, Hz
$\mathcal{F}$	shaft rotation frequency, Hz
Z	nondimensional liner impedance

R nondimensional liner resistance
X_m liner mass reactance, m
h liner thickness, m
k wave number, rad m^{-1}
Ψ test function in the weak equation
N_n FE base function
ξ, η computational coordinates in the canonical domain
i $\sqrt{-1}$

INTRODUCTION

With the expansion of major cities, increasing numbers of people live near large airports, and this leads to problems caused by aircraft noise. Recently in order to meet new noise level criteria a lot of effort has been invested by the noise control community to reduce the noise emissions from aircraft engines.

For a typical turbofan engine, fan and exhaust noise are among the major components of the noise signature of an aircraft. From the analysis of a fan engine noise spectrum it is easy to distinguish the two main components that characterize the sound, i.e. tonal and broadband noise [1]. Owing to the different nature of the two noise components it is possible to study the two phenomena separately.

In this study, in order to show the capability of a new hybrid FE/Spectral aeroacoustics code a tonal noise source is considered. Fan tones are highly dependent on the engine power or fan speed. The dominant fan tones are due to the rotor-alone pressure field, which is comprised of modes spinning with the same circumferential phase speed as the fan [2]. In fact aero-engines operating with fan tip speeds which exceed the speed of sound are known to generate an acoustic signature which contains energy spread over a wide range of harmonics of the engine shaft rotation frequency. At sub-sonic fan tip speeds, e.g. during landing, the rotor-alone pressure field attached to the ducted fan is cut-off and decays with distance upstream of the fan.

One of the most effective methods of noise reduction in turbofan aircraft engines is the use of acoustic absorbent panels, widely used in inlet and exhaust ducts, as a passive means of noise reduction. The use of a non-uniform impedance distribution offers the prospect of increasing sound attenuation without changing the engine characteristics, such as the weight. This article concerns computational methods to be used to optimize an acoustic liner for an aero-engine.

Starting from earlier papers by Rice [3] [4] [5] on acoustic liner optimization, several papers have been presented recently on this topic. In Robinson and Watson [6] a checkerboard liner optimization study for a rectangular duct is reported. In Hamilton and Astley [7] a lip liner optimization in the mid frequency range using the commercial software ACTRAN is reported. In the first instance, only a small number of propagating modes have been taken into consideration, whereas in reference [7] and in recent studies by the current authors [8] a multi-mode source which is used to approximate broadband noise forms the basis for the optimization. This latter study compared two types of axisymmetric acoustic liner configuration— a uniform and an axial liner.

The principal aim of the new work presented here is to demonstrate that it is possible to assemble a liner acoustics optimization procedure for a turbofan inlet using a new hybrid FE/Spectral code ARCADIA, see Giles et al. [9] [10]. The use of a FE code for an acoustics optimization study has been always a prohibitive task because of the computational cost for each of the design calculations. The use of a spectral discretisation in the circumferential direction means a reduction of the discrete points needed. In addition, increases in computational resources and tools available, i.e. parallel computation-grid technology [11], make this kind of optimization study feasible. The general optimization approach here used is based on the assumption that each of the steps in the optimization process can been seen as independent 'black boxes', and these can be developed and used separately. To demonstrate the capability of the optimization procedure two different test cases have been considered.

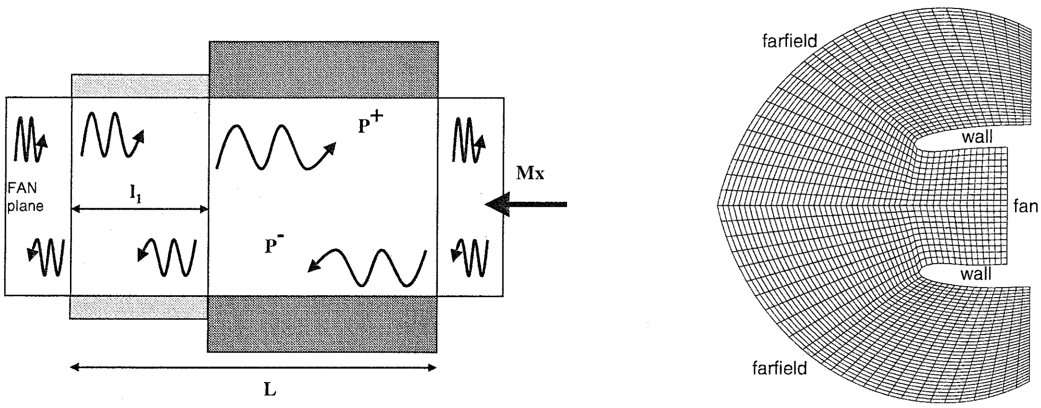

(a) (b)

Figure 1: (a) Longitudinal section of the inlet duct model. M_x indicates the flow mach number, $P^{+/-}$ are the transmitted and reflected modes, $l_1 \in [0 : L]$ is the first liner length, L is the total length of the axial liner. (b) Longitudinal section of the grid for the three dimensional scarfed nacelle test case.

ered. First a simple model of the inlet modelled by a finite length circular-section cylindrical duct is studied, see Fig.(1 (a)). In this case the optimization process uses as design variables the liner length l_i, the resistance R_i and depth h_i in each sector i. For the duct test case two different configurations are considered, a uniform liner (i.e. $l_1 = 0$) which consists of a single section of lining, and an axial varying liner consisting of two liners joined together, see Fig.1 (a). The aim is to predict the optimum liner configuration. Then the code and the design procedure have been tested with a three dimensional non-axysimmetric nacelle geometry. Fig. 1 (b) shows a longitudinal section of the nacelle geometry. In this case the design variables used are the fan relative liner position and the nacelle scarf angle, with objective function based on reducing farfield sound radiation.

The optimization procedure used here is based on Design of Experiments (DoE) methods [12] to build an ensemble of sample points, and kriging to build a Response Surface Model (RSM) [13], that is a surrogate model of the real function that will be searched instead of the real problem. The parallel capability of this method, and the use of a surrogate model, strongly reduce the runtime. The result is a reduction in the effort spent searching in areas of poor design, giving a reliable optimum using only a limited number of function evaluations.

ACOUSTIC MODEL

The acoustic model used here is based on the linearized set of equations governing the isentropic motion of a non-viscous, non-heat-conducting irrotational flow with Mach number $M_x < 1$. The steady mean flow has velocity potential ϕ. It is assumed that an unspecified noise source introduces harmonic disturbances, $\widehat{\phi}\, e^{i\omega t}$. It is found that $\widehat{\phi}$ satisfies the convected Helmholtz equation. The relative weak form is given by

$$\int_V \rho\nabla\widehat{\phi}\cdot\nabla\Psi - \frac{\rho}{c^2}\left(\nabla\phi\cdot\nabla\widehat{\phi} + i\omega\widehat{\phi}\right)(\nabla\phi\cdot\nabla\Psi - i\omega\Psi)\,dV - \int_{\partial V}\beta\Psi dS = 0, \qquad (1)$$

where

$$\beta = \rho\frac{\partial\widehat{\phi}}{\partial n} - \frac{\rho}{c^2}\left(\nabla\phi\cdot\nabla\widehat{\phi} + i\omega\widehat{\phi}\right)\frac{\partial\phi}{\partial n}. \tag{2}$$

The boundary conditions of practical interest for an engine inlet duct can be represented by a suitable choice of β [9]. The discretisation of the flow field makes use of a standard Galerkin FE representation in the axial-radial plane (ξ, η)

$$\phi(\xi,\eta) = \sum_n N_n(\xi,\eta)\phi_n, \tag{3}$$

where $N_n(\xi,\eta)$ is a shape function which has unit value at node n, and is zero at the other nodes. In the circumferential direction a discretisation has to be defined and this depends on the problem/geometry.

When an axisymmetric geometry is considered the acoustic solution is characterized by a circumferential variation $\exp(im\theta)$, where m is the specified incoming azimuthal mode due to the fan rotation. In other words a circumferential discretisation is not needed. Then using the standard multiple pure tone approximation yields

$$\widehat{\phi}(\xi,\eta,\theta) = \sum_n \exp(i\, m\, \theta)N_n(\xi,\eta)\widehat{\phi}_n. \tag{4}$$

The weak form (1) gives the linear system of equation $(\widehat{L}_0 + \widehat{F}_0)\widehat{\mathbf{\Phi}}_0 = \widehat{\mathbf{f}}_0$. The forcing term $\widehat{\mathbf{f}}_0$ is a function of the incident duct mode from the modal boundary condition on the fan face and $\widehat{F}_0$ is an operator which represents the non-reflecting condition at the exit plane (anechoic termination).

When the geometry is non-axisymmetric the assumption of mode spinning as $\exp(im\theta)$ is not valid, therefore a discretisation in θ has to be defined. Keeping the basic FE discretisation in the axial-radial plane a spectral Fourier decomposition of the solution and geometry is performed in the θ direction, yielding

$$\begin{aligned}\phi(\xi,\eta,\theta) &= \sum_j\sum_n \phi_{nj}\, N_n(\xi,\eta)\exp(i\,(j\,\theta)),\\ \widehat{\phi}(\xi,\eta,\theta) &= \sum_j\sum_n \widehat{\phi}_{nj}\, N_n(\xi,\eta)\exp(i\,(m+j)\,\theta),\end{aligned} \tag{5}$$

where the Fourier mode $j = 0$ gives the axisymmetric solution. Thus, if the unknowns are grouped by Fourier mode, then the full set of discrete equations has the form $(\widehat{L}+\widehat{F})\widehat{\mathbf{\Phi}} = \widehat{\mathbf{f}}$. The matrix $\widehat{F}$ is block diagonal with block $\widehat{F}_m$ having the appropriate boundary condition associated to the mode $m + j$. In practice the number of Fourier modes j that need to be retained is small, relative to the number of nodes in the circumferential direction which would be required by a standard 3D FE solution [10].

Now, once the basic equations and discretisation have been introduced, in order to perform a liner design study a model to predict the acoustic impedance is required. Typical acoustic liners used in current turbofan ducts consist of a perforated face-sheet bonded to a honeycomb core. There are a number of models that have been developed to use with an aeroacoustics codes to estimate the acoustic impedance of locally-reacting liners. The most common acoustic liners are single-cavity liners (SDOF — single-degree-of-freedom) and double cavity liners (2DOF — two-degree-of-freedom). The type of liner determines the specific acoustic impedance Z at the duct wall. In this work a SDOF liner model has been used [14]. The (non-dimensional) specific acoustic impedance is defined as

$$Z = R + i(km_r - \cot(kh)), \tag{6}$$

where the mass reactance m_r is taken to be a constant. The choice of using a constant mass reactance is justified by the desire to use a simple liner model that takes into account the frequency dependency. The effect of the grazing flow on the resistance value is not considered since a single flight condition, i.e. sideline, is used in all the tests. The acoustic liner boundary conditions are included in the quantity β, eq. (1), following the approach of Eversman [15] based on the Myers's model [16].

Along with the liner impedance model, a noise source representation has to be chosen. In this study only the tonal nature of the fan noise is considered. In a turbofan inlet duct the dominant fan tones are typically at harmonics of blade passing frequency (BPF). In fact when the fan tip speed is supersonic the rotor-alone pressure field is comprised of a set of modes all spinning with the same circumferential phase speed as the fan. These tones have frequency $f = m\mathcal{F}$, where $\mathcal{F}$ is the engine's shaft rotation frequency. These are known as engine order (EO) harmonics. The non-dimensional frequency is given by EO $= f/\mathcal{F} = m$. The blade passing frequency is EO $= B$. However, tones which are not harmonics of BPF also tend to have significant amplitudes at supersonic fan speeds.

Also, at supersonic fan speeds it is assumed that most of the energy at the fan plane is located in the region close to the engine case (i.e. in the first radial mode). Thus each EO tone is modelled by a single mode with azimuthal mode number m = EO and radial mode number $n = 1$. Assuming the approximation of the pressure field close to the fan plane is valid, the subsequent noise transmission and scattering is calculated by the FE/Spectral code ARCADIA.

For a given engine shaft rotation frequency all the tones that are multiples of $\mathcal{F}$ are calculated. In this study it has been possible to include the first fifty-nine engine orders in the calculations.

OPTIMIZATION METHODS

The potential noise reduction achieved by optimizing the liner or nacelle geometry is examined next. Three test cases are considered, a straight duct with two different liner configurations and a full three-dimensional nacelle geometry.

First a duct with a uniform liner is studied. This problem has two design variables which specify the acoustic liner, namely the resistance R and liner depth h. Therefore, the search is conducted in the 2D space, i.e. the (R, h)-plane. Secondly a duct with an axially-segmented liner is considered. In this case the problem has five design variables which specify the axial liner, namely R_1, R_2, h_1, h_2 and l_1. As the number of design variables is greater than two a more sophisticated and efficient optimization procedure has to be used. Finally a three dimensional non axisymmetric nacelle geometry is considered. In this case a simple optimization search is performed based on only two design variables, namely the axial position of the acoustic liner and the scarf angle.

Many optimization techniques are available, however most of these methods are time-consuming when the objective function is expensive to calculate. This means that the number of simulations (objective function evaluations) used to generate a suitable design is an important issue [17]. A relatively new optimization method is to build a surrogate model, and search this model instead. A Response Surface Model (RSM) is used here. First by running the simulations at a set of points (experimental design) and fitting response surfaces to the resulting input-output data, we obtain fast surrogates for the objective and constraint functions (if there are any), that can be used for optimization, as explained by Jones [13] and Keane [18].

The basic RSM process involves selecting a limited number of points at which the numerical simulations will be run, normally using formal DoE (Design of Experiments) methods [12]. Then, when these simulations have been performed, usually in parallel, a response surface (curve fit) is constructed through or near the data. Design optimization is then carried out on this surface to locate potential combinations of the design variables (that appear to minimize the cost function), which may then be fed back into the full code. These data points can then be used to update the model, and the whole process is repeated until some form of convergence is achieved, or an acceptable design has been obtained. There are a number of variations and refinements that may be applied to the basic

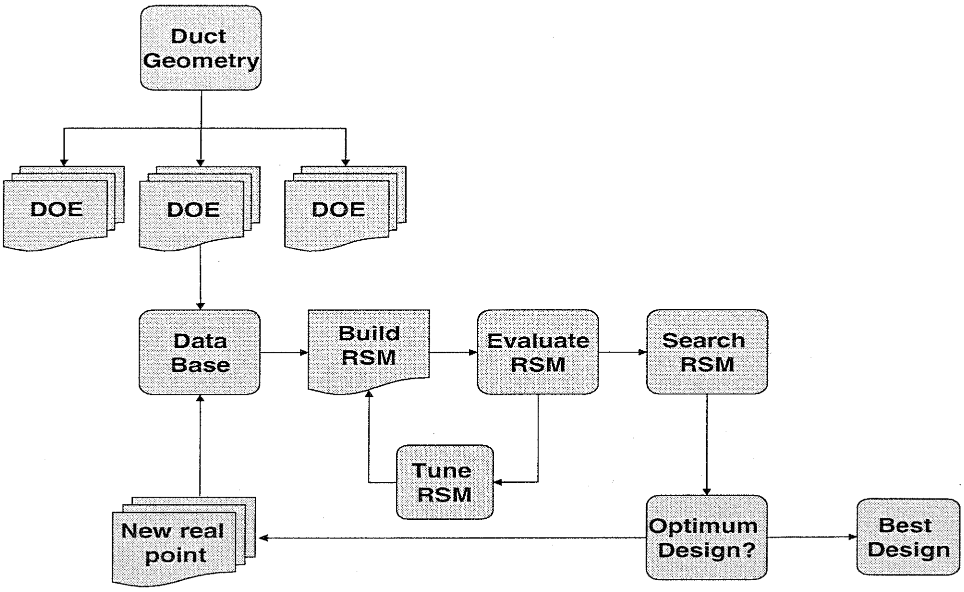

Figure 2: RSM-based optimization strategy.

RSM approach. Here the general approach used takes an LPτDoE (sequence of initial points), and then a kriging method is applied to build the RSM. Most DoE methods seek to sample the entire design space by building an array of possible designs with relatively even but not constant spacing between the points. A particular advantage of the LPτDoE approach is that it not only gives good coverage for engineering design purposes, but that it also allows additional points to be added to a design without the need to reposition existing points. Then if the initial build of the RSM is found to be inadequate, a new set of points can be inserted without invalidating the statistical character of the experiments. After the array of data points is built – from which a surface can be constructed – a decision has to be made whether to regress (as opposed to interpolate) the data. In this case the RSM model is built using a kriging approach with regularization. This method allows the user to control the amount of regression (smoothing) as well as providing a theoretically sound basis for judging the degree of curvature needed to adequately model the user's data. Kriging also provides measures of probable errors in the model being built that can be used when assessing where to place any further points. Here a two stage search (genetic algorithm (*GA*) and a gradient descent (*DHC*)) of the likelihood function has been carried out to tune the hyper parameters that define the kriging RSM. Finally a similar two stage search has been carried out on the RSM itself to find a new set of points that will be added to the database of sample points used to refine the RSM. This process is shown in Fig. 2.

COMPUTATIONAL TOOLKITS

The optimization strategy described above is both computational expensive and data intensive. It requires efficient use of computational resources and effective management of the analysis results. Grid computing technology can play an important role in exposing more computing power and allows wider accessibility of the data. In this work, several toolkits developed by the Geodise project (Grid-enabled optimization and design search for engineering) are used. [11] The Geodise project aims to provide grid solutions for engineering design optimization by removing the barriers to accessing remote computational and data resources. This is achieved by providing a set of toolkits (middleware) within the Matlab environment. These toolkits include the "compute toolkit" which can be used to submit computation jobs to Globus servers; the "database toolkit" which makes data accessible on the grid, and the "xml-toolkit" which converts Matlab data into and from xml format.

Using the toolkits, a compiled version of the ARCADIA code was submitted to the UK National Grid Service for parallel evaluation on design points obtained using design of experiments. Results including files and metadata were archived into a Grid database via Web Services interface. A hierarchical structure can be established using the datagroup concept provided by the database toolkit and this allows better management of the results. More points can be added to the same group using the update procedure. The toolkits have been used by a number of projects to better exploit the resources exposed by the Grid middleware.

RESULTS

The principal aim of this work is to assemble and demonstrate an acoustic liner/geometry design optimization procedure using the hybrid FE/Spectral code ARCADIA. Here the results for the different test cases studied are presented. The first part of the optimization study is based on an idealized turbofan engine inlet, then a real three dimensional scarfed nacelle geometry is considered, (see Fig.(1)). In both cases the mean flow and the fan's blade passing frequency (BPF) are based on a realistic flight condition, i.e. sideline (high engine power).

For all the test cases, the optimization starts by building an initial base of design points generated with a LPτDoE distribution and evaluated in parallel. The ARCADIA codes were run in parallel on the UK National Grid Services (NGS) resources using the Geodise compute toolkit and results are archived into a Grid-enabled database augmented with metadata. To cope with possible failures, a semi-automated approach was adopted, in which the computational jobs were first submitted onto the NGS with metadata related to the jobs archived into the database. At a later stage, a query process was used to poll the job and retrieve the results from scratch directories on the NGS and the results were then archived into the database. The third step involves building the response surface model based on results retrieved from the database, and an update procedure is adopted to improve this model.

Circular Duct

For the circular duct with circumferential cross-section the target of the optimization study is maximizing the sound attenuation in the duct. This is achieved by tuning some of the parameters that characterize the liner. Specifically the resistance R and liner depth h in eq. (6), whereas all the other parameters are kept constant. The design variables are searched over the range $R = [1, 10]$ and $h = [6, 60]$ mm. The objective function used to predict the liner performance is the Perceived Noise Level (PNL), as defined in the advisory circular 36-4C [19]. The PNL is defined as a function of the in-duct sound power transmission loss at the third octave center band frequencies. In this case the acoustic model takes into account the first 59 engine orders. This is sufficient to include the first eighteen octave center band frequencies.

For this geometry two different liner configurations are tested: a uniform and an axially segmented liner. For the uniform liner, a two dimensional optimization problem is conducted which searches the space $\{R, h\}$. The objective function is defined as $\Delta_{\mathrm{PNL}} = \mathrm{PNL}_{\mathrm{hw}} - \mathrm{PNL}_{\mathrm{sw}}$, which is the difference in the Perceived Noise Level for a duct with ($_{sw}$) and without ($_{hw}$) an acoustic liner.

Following the optimization procedure illustrated in Fig. 2, a sufficiently accurate response surface model is built from an initial 40 DoE sample points. In Fig. 3 the DoE sample points distribution in the $\{R, h\}$ space is shown, and in Fig. 4 the response surface built from these points and the successive update points are shown for the uniform case. It can be seen that at high engine power, the optimum Δ_{PNL} is predicted for a lining with a very high resistance, and a shallow depth.

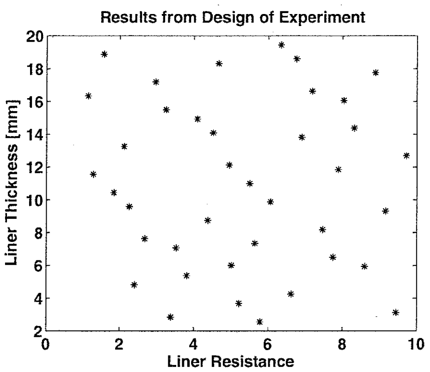

Figure 3: Design of experiments sample points distribution.

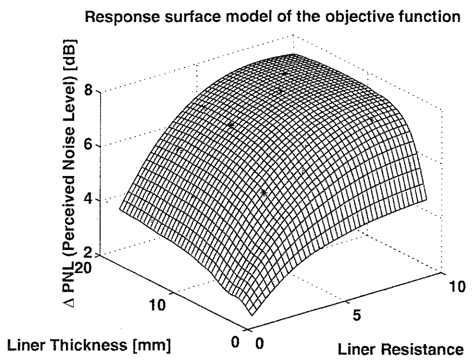

Figure 4: Responce surface model build on the initial DoE points and successive search results.

When the axial liner problem is examined a five dimensional optimization search is performed. The design variables are the resistance and depth of the two liners, and the relative length of the first liner. In this case the initial response surface is build using 160 DoE sample points. Then a double optimization process is used, first the hyper-parameters that define the kriging RSM are tuned to best fit the data, then the RSM is searched to find the improved designs. In Fig. 5 a 5D hierarchical axes technique (HAT) plot is shown. This plot contains most of the information needed to analyse the axial liner optimization.

In order to better read the 5D HAT plot a single contour subplot is first examined. The horizontal and vertical axes are h_1 and h_2 and the Δ_{PNL} contours are for a fixed value of the resistances R_1, R_2 and the relative liner length l_1/L. The next step is to look at one of the four main plots. Each of these plots is for a fixed value of l_1/L. The outer axes are the values of the liner resistance R_1 and R_2. Then at a fixed value of l_1/L and for each combination of (R_1, R_2), a single contour plot is shown for h_1 and h_2, that is $\Delta_{PNL} = \Delta_{PNL}(\mathrm{h_1, h_2, R_1 = const, R_2 = const, l_1/L = const})$. Finally viewing the overall plot, the objective function over the design space, at discrete values of resistance and length is shown. It is important to note that all the plots are on the same colour scale.

Several different optimum values can be located in the design space for different liner configurations. A liner configuration for which the objective function (ΔPNL) is maximized can be interpolated from Fig. 5. With an axially-segmented liner the optimum design (full scale engine) is about $R_1 = 6.8, R_2 = 6.3, h_1 = 20$ mm, $h_2 = 2$ mm and $l_1/L = 80\%$. The maximum predicted attenuation is $\Delta_{PNL} = 8.0$ dB, an increase in attenuation of 0.5dB compared with the uniform lining.

The optimum located for the axially-segmented liner illustrates how scattering caused by using two different liners joined together can reduce fan noise compared to using a uniform liner.

3-D Inlet

Finally, a real three dimensional nacelle geometry is used as a test case to show the capability of the optimization procedure used in combination with the ARCADIA code. Here the design variables are the relative fan liner position and the nacelle scarf angle. A single liner is used and the non

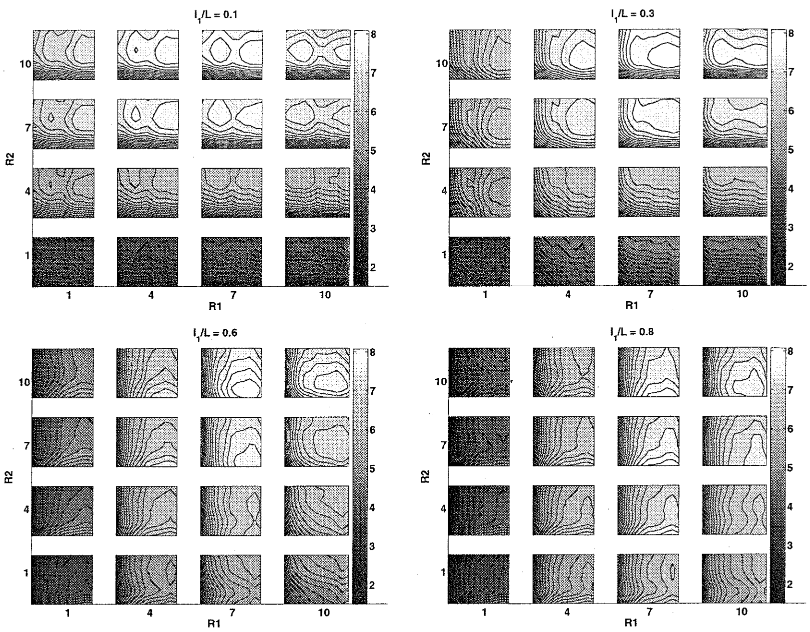

Figure 5: 5D HAT plot for an axially-segmented liner on a straight duct. It has four main blocks of contour plots, each of which contains 4x4 subplots. The subplot has axes h_1 and h_2. Each main block has axes R_1 and R_2, and corresponds to different values of l_1/L.

dimensional impedance value adopted is the optimum resistance and depth found for the uniform liner duct optimization.

Because of computational time needed for each EO using the full 3D geometry, the acoustics model only uses a single propagating mode. The mode is at BPF, and $m = B$. In this case a different objective function is used. This functional is the integral over the entire far-field boundary, see Fig. 6, of the square of the acoustic pressure weighted with $(1 - \cos(\theta))/2$, where θ is the azimuthal angle (0 at the top) such that there is more weight to the acoustic field closest to the ground.

In this example, the acoustic liner extends from 0.1 to 0.5, the axial coordinates of the liner, where 0 and 1 correspond to the inlet highlight and fan face, respectively. Fig. 6 shows different nacelle sections at different circumferential locations. Here the same optimization strategy applied to the uniform liner duct test case is used. In Fig. 7 a contour map of the function is presented. It is seen that the scarf angle and the liner position clearly affect the radiation of sound.

CONCLUSIONS

In this article the potential of a new Hybrid/FE acoustics code ARCADIA for optimization is demonstrated. The aim is to generate accurate optimization results in a reasonably short computational time for applications to aeroacoustics.

To avoid the long running time typical of acoustics FE codes, a sophisticated procedure for the optimization strategy, job submission and data parsing is assembled. The use of parallel runs, the Geodise compute toolkit for optimization, job submission and results database construction along with the spectral discretisation in the circumferential direction for a three-dimensional geometry makes this kind of problem feasible for practical application.

The assembled software can be adapted to other types of similar problems. More results are

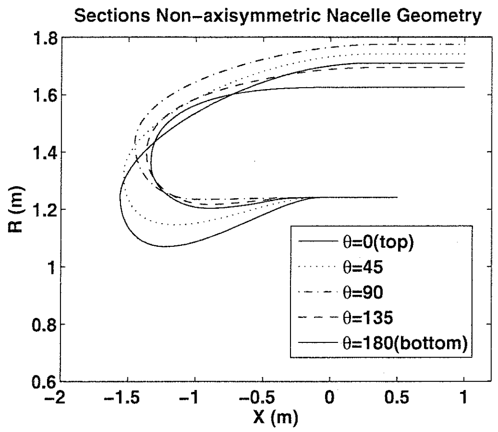

Figure 6: Inlet geometry described by a set of axial sections at different circumferential angles θ.

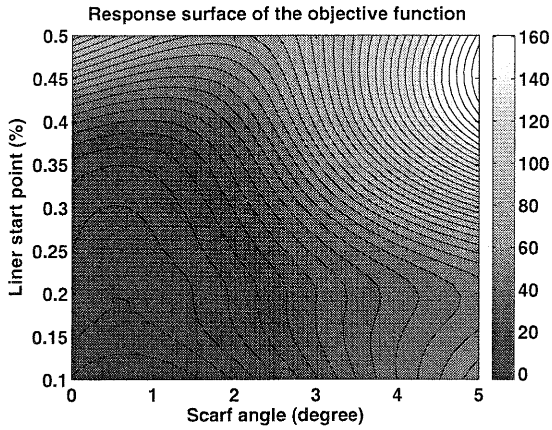

Figure 7: Functional countour plot against the two design variables, inlet scarfing angle and liner start position.

required to be able to optimize an acoustic liner for a real aero-engine. A noise source model which includes both tonal and broadband noise would also be required to conduct a realistic liner design optimization.

The next step will be to consider a realistic inlet geometry, flow and noise source model. Then the optimization could involve both the properties of the acoustic liner, and also the geometry of the inlet duct.

References

[1] Allan D. Pierce. *Acoustics - An Introduction to Its Physical Principles and Applications*. McGraw-Hill, 1981.

[2] A. McAlpine M.J. Fisher. On the prediction of "buzz-saw" noise in aero-engine inlet ducts. *Journal of Sound and Vibration*, 241(1):123–149, 2001.

[3] E.J. Rice. Optimum wall impedance for spinning modes-a correlation with mode cutoff. *Journal of Aircraft*, 16(5):336–343, 1979.

[4] E.J. Rice. Modal propagation angles in ducts with soft walls and their connection with suppressor performace. *Journal of Aircraft*, 16(5):336–343, 1979.

[5] E.J. Rice. Acoustic liner optimum impedance for spinning modes with mode cutoff ratio as design criterion. *AIAA paper 76-516*, 1979.

[6] W.R. Watson J.H. Robinson. Design and attenuation properties of periodic checkerboard liners. 12-14 May 2003-3247. Proceedings of the 9th AIAA/CEAS Aeroacoustics Conference and Exhibit, Hilton Head, South Carolina.

[7] J.A Hamilton R.J. Astley. Theoretical optimisation of an intake lip liner for a320/cfm56 flight tests. Technical Report D1.2-3.5-11, Silencer Consortium, November 2002.

[8] L. Lafronza A. McALpine A.J. Keane R.J. Astley. Computer aided liner optimization for broadband noise. 10-12 May 2004-3029. Proceedings of the 10th AIAA/CEAS Aeroacoustics Conference and Exhibit, Manchester, England.

[9] M. C. Duta M. Giles L. Lafronza. Adjoint sensitivity analysis for aeroacoustics applications. 12-14 May 2003-9328. Proceedings of the 9th AIAA/CEAS Aeroacoustics Conference and Exhibit, Hilton Head, South Carolina.

[10] M. C. Duta A. Laird M. Giles. A hybrid fe/spectral formulation of turbofan noise radiation. *International journal for numerical methods in fluids*, 4, 2004.

[11] M.H.Eres G.E.Pound Z.Jiao J.L.Wason F.Xu A.J.Keane S.J.Cox. Implementation and utilisation of a grid-enabled problem solving environment in matlab. *Future Generation Computer Systems*, In press.

[12] R.H. Jones D.C. Montgomery. *Response Surface Methodology: Process and Product Optimization Using Design of Experiments*. Wiley, New York, 1995.

[13] D.R. Jones. A taxonomy of global optimization methods based on response surfaces. *Journal of Global Optimization*, 21:345–383, 2001.

[14] R.E. Motsinger R.E. Kraft. Design performance of duct acoustic treatment. *NASA RP-1258*, 2(4):681–708, 1991.

[15] W. Eversman. The boundary condition at an impedance wall in a non-uniform duct with potential nean flow. *Journal of Sound and Vibration*, 246(1):63–69, 2000.

[16] M. K. Myers. On the acoustic boundary condition in the presence of flow. *Journal of Sound and Vibration*, 71:429–434, 1980.

[17] D.R. Jones M. Schlonlau W.J. Welch. Efficient global optimization of expensive black-box functions. *Journal of Global Optimization*, 13:445–492, 1998.

[18] A.J. Keane. *The Options design exploration system Reference manual and user guide*. 2002.

[19] U.S. Department of Transportation Federal Aviation. Noise standard: Aircraft type and airworthiness certification, 7-2003. Advisory Circular AC36-4C.